

Chapter 3

Photoelectron diffraction study of the Ni(100)c(2x2)-N₂ system

Despite the catalytic importance of nitrogen in the formation of ammonia, the study of the adsorption of N₂ on a Ni(100) surface cannot be justified from the point of view of its catalytic interest. As discussed in the introduction of this work, in order to be of catalytic relevance, molecular nitrogen should first dissociate into atomic nitrogen. However, on a Ni(100) surface dinitrogen adsorbs molecularly.

Nevertheless such a system is of a true significance. While the general understanding of interatomic bond lengths in molecular systems has been well established for many years [22], and some of the general concepts of bond order have been proved to be rather effective in the description of atomic chemisorption at metal surfaces [23,24], less attention has been paid to understanding bond lengths associated with molecular chemisorption at metal surfaces. In this respect, the study of adsorption of simple molecules on metal surfaces should serve as a model to understand the fundamentals of the interaction amongst molecular adsorbates and surfaces. Indeed, the adsorption of carbon monoxide (CO) on different transition metals has been generally used as a prototype system for studying molecular adsorption, whereas there are considerably fewer studies on the adsorption of the isoelectronic molecule N₂ on metal surfaces. However, in spite of the similarities between both molecules, their behaviour upon adsorption can be rather distinct. For instance, on nickel surfaces CO forms a somewhat strong chemisorption bond, while N₂ adsorbs more weakly. This is not surprising as most of the individual orbitals are quite different (for example, the unoccupied CO 2π* orbital has much more weight toward the carbon end, where the metal atom is known to be bonded, while the equivalent orbital is symmetrically distributed between the two N atom in the N₂ molecule). Thus, the study of the adsorption of molecular nitrogen on nickel surfaces should provide some hints about the differences between strong and weak chemisorption.

It also has to be considered that to have knowledge of accurate structural data on the adsorption of molecules on surfaces is essential to support any possible theoretical description of the adsorbate-surface chemical bond. For instance, various attempts to interpret the bonding between N₂ and a Ni(100) give different descriptions of the electronic

ground state of the system, in which corresponding bonding distances differ by six tenths of an Ångstrom [25, 26].

Moreover the N 1s photoemission spectrum of the Ni(100)c(2x2)-N₂ surface presents some interesting particularities. Molecular nitrogen is known to adsorb on Ni(100) in an end-on configuration, rendering the two N atoms inequivalent. This situation is reflected in the N 1s photoemission spectrum (see Fig. 3.1), where two distinct chemically shifted components are identified as originating from these two (now inequivalent) N atoms of the dinitrogen molecule. Furthermore an unusually intense satellite structure, a so called “giant satellite”, appears at lower kinetic energy than the two main adiabatic peaks. Although this issue of the multielectron excitations in the XPS final state of N 1s emission from N₂ adsorbed on Ni surfaces has been the subject of a considerable amount of both experimental and theoretical studies [25, 27–40], a consensus on its physical origin has not yet been attained.

The aim of the present study was first to obtain the necessary structural information about the Ni(100)c(2x2)-N₂ system in order to cast light on the trends in bond lengths between molecules and surfaces. As the N atoms are chemically inequivalent by the end-bonding to the Ni(100) surface, independent structural information on the two ends of the molecule can be extracted if the experimental resolution is good enough to resolve both N 1s photoemission components. Actually one of the purposes of this work was to test if it would be possible to perform Chemical Shift Photoelectron Diffraction experiments at the BESSY II synchrotron facility in Berlin on a reasonable timescale and with the required energy resolution¹.

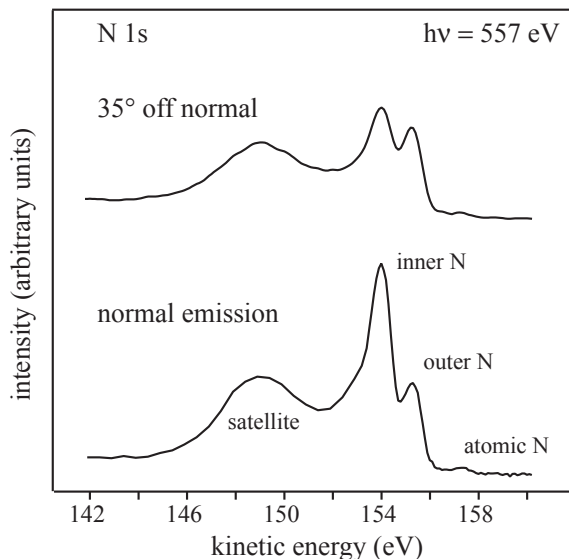


Figure 3.1: N 1s core level photoemission spectra measure at normal emission and 35° off normal emission

¹The experiment was performed on June 2000 during one of the first beamtimes of our group at BESSY II

Another aspiration of this work was to acquire some further understanding of the character of the “giant satellite” structure that appears in the N 1s photoemission spectrum from variations in its intensity in different emission directions.

3.1 Adsorption structure

Molecular nitrogen is known to chemisorb weakly on Ni(100) with an isosteric adsorption energy of approximately $40 \text{ kJ}\cdot\text{mol}^{-1}$ at low coverages and at low temperatures forms a 0.5 ML ordered $c(2\times 2)$ surface phase² [41]. The first work on the orientation of the dinitrogen molecule upon adsorption on a Ni(100) surface, based on NEXAFS experiments [42], pointed to a standing-up geometry in which the molecular axis is perpendicular to the surface. This result was endorsed by an ARUPS experiment [43] in which only two features were observed at $\bar{\Gamma}$ when s-polarized light was used, while any other orientation of the molecule would have resulted in more than two features under such conditions. The upright orientation was also confirmed by X-ray photoelectron diffraction experiments [30, 44]. In these XPD experiments the emission from the N 1s level was measured at different emission geometries resulting in a different angular dependence of the photoemission intensity of the two main adiabatic components of the spectrum. At normal emission the adiabatic component with the lowest kinetic energy presented an enhancement of its intensity, which vanished when the spectrum was measured at off-normal polar angles. Since for photoelectrons with high kinetic energy the photoemission intensity from an atom would be heightened by the presence of an atom in front of it due to forward elastic scattering [45], the component with the lowest kinetic energy can be identified as due to emission from the “inner” N, the one located closer to the Ni substrate, forward scattered off the “outer” N, situated directly above it. This behaviour can be seen in Fig. 3.1 where the N 1s spectra measured in the present experiment for normal and off-normal emission are shown.

This component assignment agrees with a prior analysis based on the *equivalent-core approximation* (ECA) [46] of the possible photoemission final states for the present system. The ECA considers that, since the core electrons are located almost completely inside the valence electrons, the effect on the valence electrons of a core ionisation will be practically the same as if a unit charge were added to the nucleus. Therefore, many of the properties of a core ionised atom should be the same as the properties of the next element in the periodic table³. Within this approximation, a N atom with a fully screened core hole can be equated to an oxygen atom. Thus the ECA two final states for the N_2 molecule can be represented by a NO molecule bonded to the surface via the O atom, which would correspond with a core-hole located in the inner N, or via the N atom, representing a core-hole located in the outer N. Bearing this in mind, the component with higher kinetic energy can be assigned to the outer N since the nitrogen-end down orientation for the

²The $c(2\times 2)$ can be first observed at half this saturation coverage

³This approximation is also called the *Z+1 approximation*

equivalent-core molecule NO is known to be the preferred or lower energy state [47]. Posterior ARPEFS [37] measurements are also in agreement with an orientation in which the N-N bond is normal to the Ni(100) surface.

Regarding the adsorption site, equilibrium studies [41] as well as TDS experiments [48] were consistent with a single adsorption site and ARPEFS measurements indicated this to be an atop site [37]. Furthermore, the value of the N-N stretching for molecular nitrogen on Ni(100) [49] is essentially identical to that observed on Ni(111) on which it was argued that the adsorption must be atop a single surface Ni atom [50].

So far, the only quantitative structural study of the Ni(100)c(2x2)-N₂ adsorption system is the ARPEFS study by Moler et al. mentioned above. We should note that although the authors used the acronym ARPEFS (angle-resolved photoemission extended fine structure), this technique is essentially identical to the scanned-energy mode photoelectron diffraction used in our work. This study was based on only a single N 1s photoelectron diffraction spectrum in which no chemical-state resolution of the photoemission components corresponding to the two inequivalent N atoms was attained. A multiple scattering analysis of the experimental modulation data led to the determination of some of the structural parameters of this system such as the Ni-N bonding distance, 2.25 Å, the N-N bond length, 1.10 Å, the first Ni-Ni layer spacing, 1.76 Å, as well as some non-structural parameters like the inner potential, 15.1 eV. Despite of the fact that the value of 2.25 Å obtained in this experiment for the molecule-surface bond distance agrees with the general idea that associates longer bond distances to weaker bonds, it appears to be longer than expected if it is compared with distances in metal coordination compounds involving dinitrogen. In fact, it has to be stressed that there is a lack of data to sustain a quantitative assessment of the extent to which weak bonds between molecules and surfaces are longer than strong ones. We should also remark on the value of the intramolecular distance between the two N atoms obtained by Moler and co-workers. Since no chemical-state resolution of the two N emitters was achieved in their study, no precise determination of the N-N distance could be expected. Actually, they found the N-N bond length to be the gas phase N₂ value, while is hard to imagine that chemisorption, even if weak, would not affect at all the internal bonding between both nitrogen atoms. In the gas phase the molecular orbitals are symmetrically distributed between the two centers, and upon adsorption the interaction with the metal will cause a polarisation and reorganisation of these orbitals, leading to structural changes within the molecule. Indeed, a small increase with respect to the gas phase bond length is to be expected upon adsorption due to the effect of partial occupation of the molecular antibonding 2π* level as a result of the interaction with the Ni substrate [51]. As will be discuss later, this expansion of the intramolecular N-N distance is, however, marginally significant.

In the next few sections we present the results of applying the photoelectron diffraction technique to the study of the structure of the Ni(100)c(2x2)-N₂ surface. It will be demonstrated that the previous quantitative structural study by Moler et al. was seriously mistaken.

3.1.1 Description of the experiment

The Ni(100) crystal was cleaned in the UHV system described in chapter 2 by several cycles of sputtering with Ne^+ ions followed by annealing to a temperature of 900 K. After this procedure XPS showed a low level of carbon contamination which was successfully removed by several cycles of annealing to 600 K in an oxygen atmosphere of 1×10^{-7} mbar followed by flashing to 800 K. The surface order was verified by the quality of the (1x1) LEED pattern and the cleanness of the surface was checked by XPS using the synchrotron radiation. The Ni(100)c(2x2)-N₂ surface was then prepared by exposing the surface to molecular nitrogen at 1×10^{-7} mbar while cooling slowly the sample from 150 K to 75 K using a liquid Helium reservoir connected with the sample by a copper bride. This dosing procedure assures the greatest possible ordering⁴ of the c(2x2)-N₂ overlayer. Afterwards the sample presented a clear c(2x2) LEED pattern and a N 1s photoemission spectrum typical of this system (see Fig. 3.1) which consisted of three main features: two clearly-resolved peaks, with a splitting of approximately 1.3 eV [30], associated with the adiabatic emission peaks from the two inequivalent N atoms, and a broad many-electron-excited satellite feature at approximately 6 eV lower kinetic energy than the main lines. The other weak feature to appear in the N 1s spectrum shown in Fig. 3.1 corresponds to N 1s emission from atomic nitrogen on the surface due to a small amount of dissociation. The quantity of the atomic nitrogen present on the surface did vary slightly in different preparations, in some cases being scarcely detectable, and accounts at the very most for a very small amount (1-2 %) of the total nitrogen coverage. This is unlikely to have any influence on the local structure of the molecular nitrogen adsorbate. It has to be noticed too that because of the substantial chemical shift in the photoelectron binding energy (around 2 eV) this feature does not contribute to the measured photoelectron diffraction spectra on which the structure determination will be based.

The UHV system was attached to the undulator beamline UE49-1 at the BESSY II synchrotron radiation facility in Berlin. The undulator gap could be stepped synchronously with the spherical grating monochromator, allowing the use of the peak of the third harmonic undulator radiation throughout the measurement of the energy-scanned N 1s photoelectron diffraction spectra. The photoelectron diffraction spectra were taken in the photon energy range of 480-800 eV in photon energy steps of 4 eV in a total of 11 different emission directions. Due to the intense photon flux available at the beamline, the amount of atomic nitrogen present on the surface increased slightly as the experiment progressed. For this reason the surface needed to be re-prepared every 8 hours, which allowed us to measure from 2 to 3 PhD spectra for each preparation.

⁴i.e. N₂ adsorbed into ordered approx. 34 Å wide domains [43]

3.1.2 Structural determination

The experimental chemical-state-resolved N 1s photoelectron diffraction spectra are shown in Fig. 3.2. From a first inspection of these data some primary information can be extracted. The spectra recorded at normal and close to normal emission present rather large modulation amplitudes. Such strong modulations are usually obtained when a scatterer atom is directly behind the emitter, i.e. they correspond to a near atop adsorption geometry. A surprising detail is that the modulation amplitude showed by the PhD spectra corresponding to the outer N is larger (even larger than those shown by the inner N) than would be expected for an atom which is supposed to be at a fairly long distance from the Ni substrate and therefore from the main scatterer. This aspect will be discussed in detail in section 3.2. One more piece of information that can be obtained from this qualitative examination of the data concern the relative position of the two N atoms with respect to the surface. The modulations of the inner N spectra have a larger period than those present in the outer N spectra. For instance the normal emission spectrum of the inner N contains three oscillations in the kinetic energy range from 60 to 400 eV while the respective spectrum of the outer N has four. This observation implies a closer proximity to the Ni scatterer for the inner N, which further supports the nomenclature adopted to refer to the two N atoms. For a more accurate analysis of the structural properties of the Ni(100)c(2x2)-N₂ system, the two-step procedure described in chapter 2 should be applied.

Projection method

To obtain a semi-quantitative estimate of the adsorption site, the projection method of direct data inversion was applied to the PhD spectra from the two inequivalent N atoms. The results of applying this technique to the PhD data set corresponding to each N atom are shown in Fig. 3.3. The upper panels show sections perpendicular to the surface in the [010] azimuth passing through the relevant emitter at (0,0,0); a single streaked feature is seen directly below the emitter for both cases at depths roughly consistent with the expected location of the nearest-neighbour Ni atom for an atop adsorption site. This picture is confirmed in the lower panels where sections parallel to the surface at depths below the emitters of 1.85 Å for the inner N and 3.05 Å for the outer N chosen to intersect the peak seen in the perpendicular section are shown. The single sharp feature in both cases confirms the atop or near-atop geometry. The difference in N-Ni distance for the two N atoms is 1.20 Å, fairly close to the expected value of the intramolecular N-N distance.

Notice that the “image” obtained from the outer N emitter, which is more diffuse than the one obtained from the inner N due to the longer distance to the nearest-neighbour Ni atom, does not show any feature corresponding to the location of the inner N. This result is not totally unexpected as the method is designed to exploit strong near-neighbour scattering, and the Ni atom is a strong scatterer in comparison to the nearest neighbour N atom particularly in the backward direction, where the electron scattering factor amplitude for the Ni atom presents a peak all over the energy range in which our measurements were

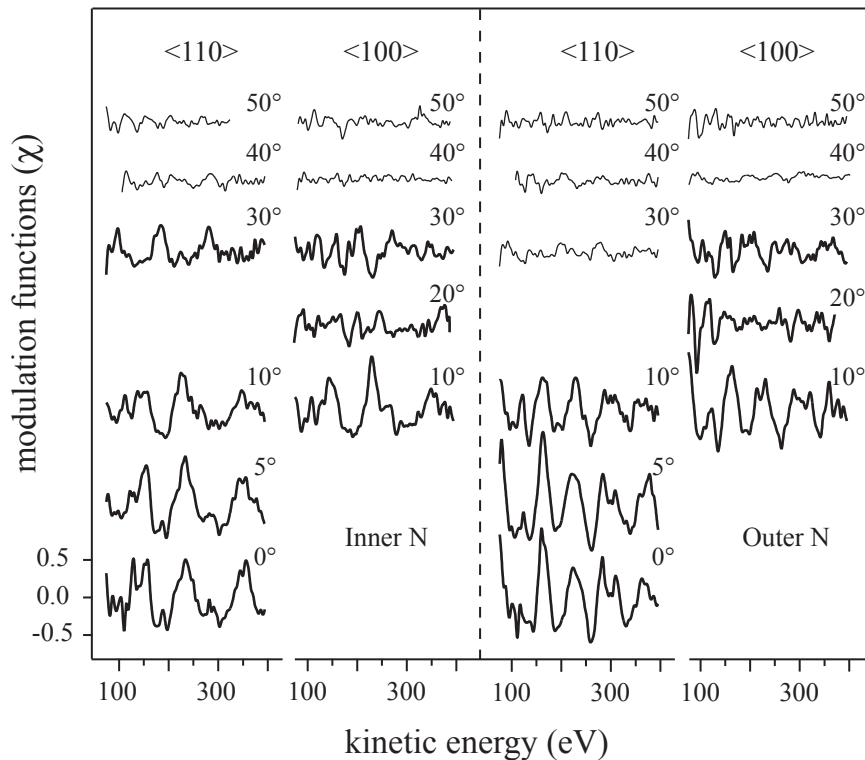


Figure 3.2: Full data-set of chemical-state-resolved N 1s PhD spectra. The spectra used in the multiple-scattering calculations are represented with bold lines

performed. In fact, the surprising result is that the Ni atom is so effectively imaged in the projection method although its distance to the emitter is rather large. This is directly related to the already mentioned large modulation amplitudes showed by the PhD spectra for the outer N. We shall see later that both features have to do with an enhancement of the backscattering contribution from the Ni atom by multiple scattering from the inner N.

Photoelectron diffraction structure determination

Although the results of the projection method point clearly to an atop adsorption geometry, in good agreement with the arguments stated at the beginning of this section and with the ARPEFS study by Moler et al. [37], multiple scattering test calculations were run for the other high-symmetry adsorption sites (hollow and bridge) as well as for a possible atop adsorption on a Ni atom of the second layer. None of these attempts gave good agreement with experiment.

Once these other adsorption sites were discarded, the structural parameters associated with the atop site were optimised. The initial calculations for the atop geometry assumed that the N-N axis was perpendicular to the surface with the intramolecular bond length equal to that in the gas phase and allowed only the variation of the N-Ni distance. Fur-

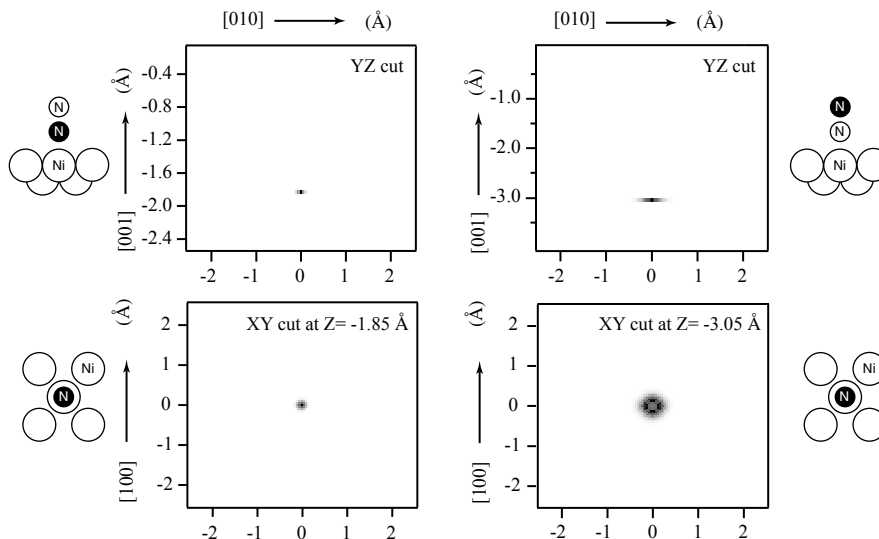


Figure 3.3: Results of the application of the direct method to the PhD modulation spectra from the inner (right panels) and outer (left panels) N emitters. Grey-scale maps show the darkest features in positions most likely to correspond to locations of Ni substrate atoms relative to the N emitters located at (0,0,0). The upper panels show sections perpendicular to the surface passing through the emitter, while the lower panels show sections parallel to the surface at a depth below the emitter chosen to cut the main feature seen in the perpendicular sections.

ther improvements were achieved by varying several other parameters including the N-N spacing, the N-N tilt and Ni-N tilt angles, the Ni-Ni layer distances in both the outermost layer and in the bulk, the inner potential and the vibrational amplitudes of each of the N emitters and the Ni surface.

Fig. 3.4 shows the comparison of the experimental chemical-state-resolved N 1s photoelectron diffraction spectra from the Ni(100)c(2x2)-N₂ surface with the results of the simulations for the best-fit structure shown schematically in Fig. 3.5. A total of nine spectra measured at high off-normal polar angles (30° and more) were removed from the data set because they showed either very weak (less than 5 per cent) or no modulation. In Table 3.1 are listed the best-fit values for the parameters used in the calculations together with their associated precision estimates.

The agreement between theory and experiment is visibly very good, although the related R-factor value of 0.23 seems to be somewhat larger than might be expected for such a good agreement. This apparent incongruity between qualitative and quantitative evaluation of the agreement between the theoretical calculations and the experimental data appears to result from the inclusion of the spectra at larger emission angles (20° and 30°) in which the modulations are weak and comparably good fits are not to be expected.

The optimal value of the inner potential was 15 eV, even though the large error (of a 40 %) associated with the determination of this parameter implies that the sensitivity of the simulations to it was rather low. The best fit values of the mean square vibrational amplitudes for the Ni and outer N atoms respectively were 0.003 Å² and 0.04 Å², while

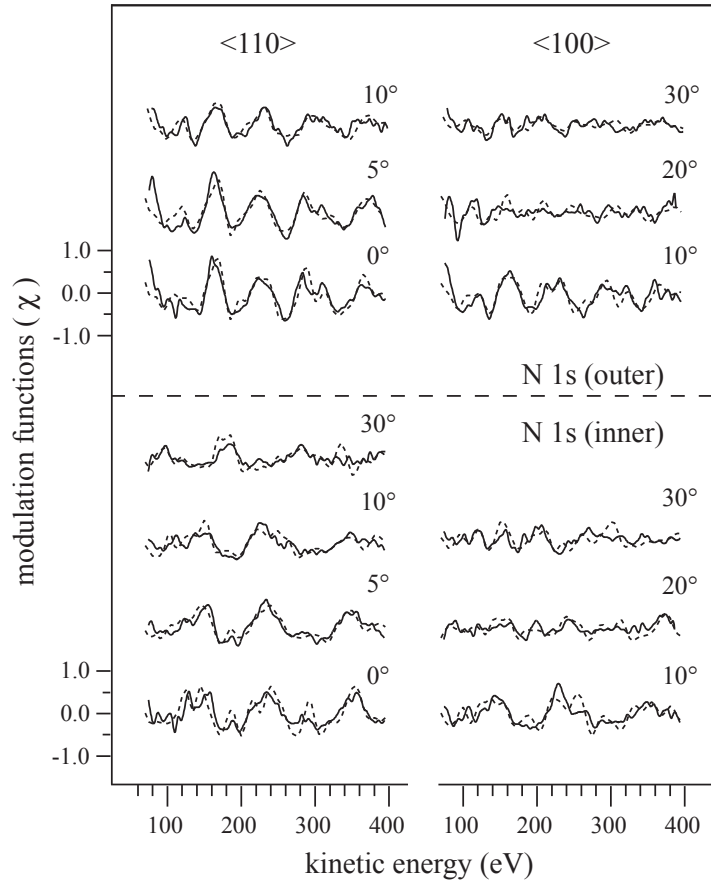


Figure 3.4: Comparison of the experimental chemical-state-resolved N 1s PhD spectra (thin lines) with the results of multiple scattering calculations (dashed lines) for the best-fit structure shown schematically in Fig. 3.5 using the parameters listed in Table 3.1

for the inner N emitter anisotropic vibrations were found to be necessary with a value of 0.01 \AA^2 parallel to the surface, but one order of magnitude smaller perpendicular to the surface. The value of 0.003 \AA^2 obtained for the Ni atoms of the substrate corresponds with a Debye temperature of 254 K which is comparable with the value of 220 K used by Moler et al. in their simulations and noticeably lower than the bulk value of 390 K [52]. This difference between surface and bulk Debye temperatures is due to an increase relative to the bulk value of the vibrational amplitudes of surface atoms [53, 54]. Indeed, while the mean square amplitudes perpendicular to the surface are almost independent of the crystallographic orientation of the surface, those parallel to the surface are larger on more open-packed surfaces. Due to this, different Debye temperatures for different crystallographic faces of Ni have been found, being 320 K for Ni(111) [55] and 220 K [56] for the more open face (110). Having this in mind, the Debye temperature for a (100) Ni surface should lie between the two temperatures mentioned above, since the surface atomic density of the (100) surface for an fcc crystal such as Ni is lower than that of the (111) face, but higher than that corresponding to a (110) surface. Although the value

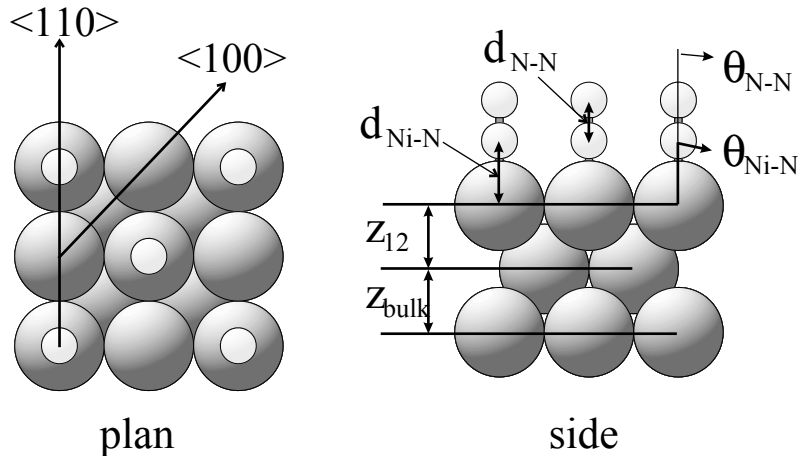


Figure 3.5: Schematic diagram of the best-fit structure for the Ni(100)c(2x2)-N₂ surface showing the definition of the principal structural parameters and the azimuthal directions in which the PhD data were collected

Parameters	CS-PhD	DFT	Moler et al.
$d_{\text{Ni-N}}(\text{\AA})$	1.81 ± 0.02	1.79	2.25 ± 0.01
$d_{\text{N-N}}(\text{\AA})$	1.13 ± 0.03	1.17	1.10 ± 0.07
$z_{1-2}(\text{\AA})$	1.78 ± 0.06	1.86	1.76 ± 0.04
$z_{\text{bulk}}(\text{\AA})$	1.76 ± 0.20	1.76	-
$\theta_{\text{Ni-N}}(\text{deg})$	0 ± 10	-	-
$\theta_{\text{N-N}}(\text{deg})$	0 ± 5	-	-

Table 3.1: Comparison between the optimum main parameter values obtained in this study and those found in the earlier work by Moler et al. [37]

we found, 254 K, fits this trend, to get an accurate value of the Debye temperature for the Ni(100) surface a thorough temperature-dependent PhD (or LEED) study would be necessary.

Since PhD is sensitive to the *relative* vibrational amplitude of the scatterers with respect to the emitters, the smaller value for the inner N atom, particularly perpendicular to the surface, could reflect the greater influence of vibrational correlations with the nearest neighbour Ni scatterer than will occur for the outer N atom as an emitter. In spite of that, the optimum values for the N vibrational amplitudes are rather large, possibly reflecting a soft vibrational mode in this structure which was actually inferred from thermodynamic measurements [41]. It should be emphasized, however, that the accuracy with which these vibrational parameters can be determined in PhD is invariably poor (typically approximately equal to the values themselves).

We have not investigated the subsurface Ni interlayer spacings in detail. The reason is that the modulations in PhD are most strongly influenced by the near neighbour scatterers, and this implies that the structural fits are relatively insensitive to the location

of the more Ni distant atoms. This is especially true for a situation of atop adsorption in which strong backscattering is typically seen only near normal emission and is dominated by the nearest neighbour Ni atom position relative to the emitters. Therefore we have assumed that while the outermost Ni layer spacing, z_{1-2} , may differ from the bulk spacing, all other subsurface layer spacings are the same. The value we obtained for the Ni-Ni spacing between the two first layers is slightly larger than the value obtained for the bulk layer spacing that matches the actual bulk nickel value of 1.76 Å. The large error estimated for the bulk layer spacing confirms that our sensitivity to it is very low.

The Ni-N distance of 1.81 Å obtained in the current work, which agrees with the result we have obtained with the projection method, differs very considerably from the previous value of 2.25 Å published by Moler et al. [37]. This difference of various tenths of an Ångstrom is extremely important from the chemical point of view bearing in mind that even a bond length change of a few hundredths of an Ångstrom has significant implications for the molecule-metal bonding character.

Nevertheless the value of the Ni-N distance obtained by Moler et al. is in agreement with the belief that weak bonds should be longer than strong ones as we have already mentioned. Because one of the aims of the present work was to try to elucidate the validity of this statement, an important part of the present study was devoted to trying to understand this discrepancy. As was mentioned in the introduction of this section, the analysis made by Moler et al. was based on a single non-chemical-state-resolved N 1s photoelectron diffraction spectrum. This spectrum was measured at 5° off normal emission and in the [110] azimuth. A single unresolved experimental photoelectron spectrum measured in the same emission direction was created from our data by adding together the intensities corresponding to the inner and outer nitrogen spectra over the same energy range as the data of Moler et al. The resulting spectrum was then normalised to obtain the modulation function and this was analysed using the values obtained in Moler's work for all structural parameters other than the inner Ni-N distance which was varied. In Fig. 3.6 the variation of the R-factor for this spectrum alone as a function of the Ni-N distance is shown. The figure shows two clear local minima in the R-factor at Ni-N distances of approximately 1.8 Å and 2.2 Å and another two at unreasonable bond-distances of 1.4 Å and 2.7 Å. From the figure it is clear that a lower R-factor is obtained for the bond length at 1.8 Å.

This problem of the appearance of multiple local minima in fitting the experimental spectra is well known both in PhD [57] and LEED [58] and it can be simply understood by considering the case of fitting a single PhD spectrum such as one of those measured at near normal emission. It has already been mentioned that such spectra are dominated by a single periodicity arising from the backscattering of the nearest neighbour substrate atom, so the period would reflect the path length difference in travelling to this scatterer and back in the 180° scattering geometry. If this path length is increased, the periodicity of the modulations will decrease continuously. However, the data presented in Fig. 3.4 cover a relative short range of energy, which typically includes only 3-4 oscillations for a nearest neighbour scatterer as in the case of the inner N. A continuous change in the

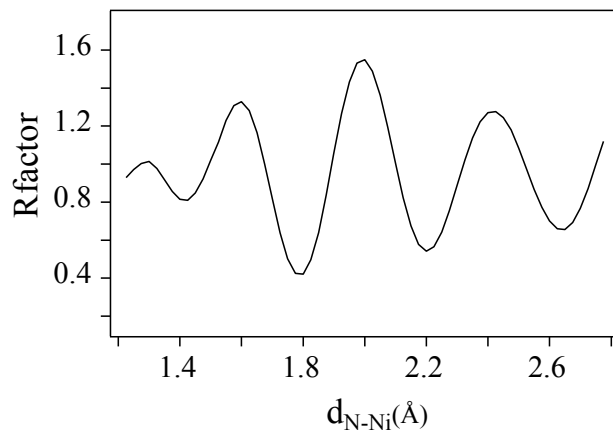


Figure 3.6: Variation of the R-factor with the parameter $d_{\text{N-Ni}}$ for the single 5° [110] spectrum with the two chemically shifted components added together to simulate a single unresolved PhD (The structural values used in this simulation were those published by Moler et al. [37])

period will therefore at first produce the experimental and theoretical modulations to shift out of phase, leading to anti-correlation and an R-factor greater than unity, but further change will result in the two curves coming back into *approximate* registry, just because a similar number of complete oscillations, though of slightly too short a period, will occur. Clearly several such approximate matches may occur in the period and phase of the dominant oscillations, albeit only one of these should match exactly in period and thus should give the lowest R-factor value. In order to suppress this problem, in LEED it is usual to improve the uniqueness of the solution by using a larger data set.

Fig. 3.7 shows the variation of the R-factor as a function of the N-Ni distance for three different data sets. The thin line is the same curve shown in Fig. 3.6 but plotted in a region of plausible Ni-N bonding distances. The bold line corresponds with a simulation for the full chemical-state-resolved PhD data set measured in the present study. The third curve shown in Fig. 3.7 (dashed line) results from similar calculations conducted for the actual data of Moler et al., digitised from the spectrum shown in their paper. As can be seen, extending the data set to the full collection of PhD spectra led to a substantially lower R-factor for the shorter bond length (parameter values are now 0.23 and 0.49 for the 1.8 Å and 2.25 Å respectively, which differ by more than ten times the estimated variance of 0.023). Notice that the simulation based on the published data of Moler et al. also shows the fit at the shorter bond length to be better and presents an even stronger preference for the shorter bond length than our own simulation of their restricted data set. Note that the R-factor used by Moler et al has a different normalisation [59], but this should have only a minor influence.

In order to provide an entirely independent check on the value of $d_{\text{N-Ni}}$ DFT calculations were conducted by Dr. Jim Robinson at Warwick University. These calculations yielded a value for $d_{\text{N-Ni}}$ of 1.79 Å, in excellent agreement with the value obtained in the present work by means of photoelectron diffraction technique (see discussion below).

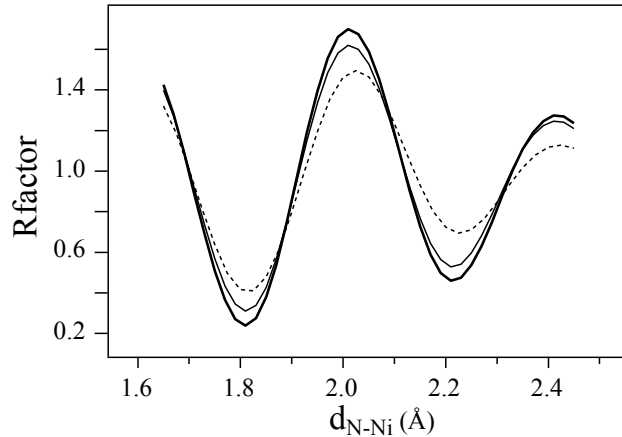


Figure 3.7: Variation of the R-factor with the parameter $d_{\text{N-Ni}}$ for three data sets: bold line - the full chemical-state-resolved PhD data set measured in the present study; thin line - the single 5° [110] emission spectrum with the two chemically shifted components added to simulate a single unresolved PhD; dashed line - single 5° [110] unresolved PhD spectrum taken from the paper by Moler et al. [37]

A further discrepancy between the results published by Moler et al. and those of the current work is the value of the N-N distance. While in Moler’s work an optimised intramolecular distance between nitrogen atoms of $1.10 \pm 0.07 \text{ \AA}$ is reported, similar to that in the gas phase, our results point to a slightly larger distance of $1.13 \pm 0.03 \text{ \AA}$. It should be stressed that in Moler’s study no chemical-state resolution of the two N emitters was achieved and no precise determination of the N-N distance could be expected. In the current work separate PhD spectra from the outer N atom have been obtained, providing a far more favorable situation to determine the intramolecular distance of this atom relative to the nearest Ni backscatterer and thus the N-N bond length. The precision with which this distance can be determined is enhanced by the fact that the modulation amplitude of the outer N PhD spectra is very large, yet as we have already mentioned this large amplitude is rather surprising.

Actually the small expansion of the intramolecular distance observed here agrees with the predictions of Blyholder’s description of the bonding, which is based on σ donation to the metal combined with backdonation from a metal d-orbital into the unoccupied $2\pi^*$ level of the N_2 molecule. This charge transfer should decrease the intramolecular bond strength leading to an increase of the N-N bond length and to a softening of the intramolecular stretching mode. Indeed, such a softening in the stretching frequency has been observed [49]. Moreover, Stöhr and Jaeger deduced from resonance shifts observed in the NEXAFS spectrum upon chemisorption of the isoelectronic CO molecule on a Ni(100) surface, an increase of the intramolecular bond length (relative to that in the gas phase) of the order of 0.03 \AA [42]. In this work a smaller resonance shift is obtained in the case of the Ni(100)c(2x2)- N_2 system, which would imply a smaller extension of the intramolecular bond length of N_2 in comparison with the value found in the CO case.

It has to be stressed, however, that the validity of the Blyholder picture, in which the molecule is treated as a unity and only the interaction of the gas phase HOMO and LUMO orbitals with the metal is considered, has been questioned by some recent work based in X-ray emission spectroscopy measurements. By using XES, the authors were able to achieve atom specific separation of the valence electronic states, so that the molecular contributions to the surface chemical bond could be separated from those of the substrate [60]. In order to understand this new piece of information, DFT calculations were carried on the basis that the gas-phase molecular-orbital approach is no longer meaningful [61]. The description of the chemical bond given in this work is different from the traditional Blyholder model in that it involves all molecular orbitals and the resulting binding energy is obtained from a balance between repulsion in the σ system and bonding based on the π orbitals. According to this model, no net intramolecular bond length change is expected. Nevertheless, this new model relies heavily on *ab initio* calculations yet never mentions the associated geometrical parameters.

Density functional theory structural determination

The DFT calculations were performed by Dr. Jim Robinson from the University of Warwick. Their results are closely related with the present discussion and therefore are included in the present work.

In view of the discrepancies between the results presented in the section above and those obtained by Moler et al., independent DFT calculations were performed addressing the question of the optimum N-N, Ni-N and Ni-Ni bond distances for N₂ adsorbed atop Ni atoms in a Ni(100)c(2x2)-N₂ structure with its N-N axis perpendicular to the surface; neither the total energies of other bonding sites, nor the possibility of molecular tilt were explored.

The DFT calculations⁵ used the CASTEP computer code [63,64], aided by the CERIOUS graphical front-end [65]. The surface net parameters used in the slabs were those found to give the minimum energy for bulk fcc Ni (which were 1.7 % larger than the experimental value). Electron spin was explicitly included in all the final optimisations, although the main influence of spin was in relative total energies rather than in the optimal geometry, so more rapid calculations on the adsorption system were performed on a c(2x2) structure using slabs comprising 5 Ni layers with the N₂ molecules adsorbed on one side of the slab in a perpendicular atop geometry. The three Ni layers furthest from the adsorbate-covered face were constrained to the calculated bulk structure, while the outermost two Ni layers were allowed to relax to their minimum energy configuration within the constraints of the space group symmetry. Calculations on the clean surface slabs, similarly constrained in the structure of one face, were conducted in order to obtain an estimate of the adsorption energy.

The structural parameters of the optimised surface geometry obtained in these calculations are summarised in table 3.1. Clearly there is rather good agreement with the present

⁵A more detailed description of the DFT calculations can be found in [62]

PhD experiments regarding the key parameter of the N-Ni nearest neighbour distance. The N-N distance of 1.17 Å appear to be significantly larger than both the gas-phase value and the value obtained by the PhD measurements, but a more proper comparison with the value obtained by the same DFT calculational procedure for an isolated N₂ species, which was 1.15 Å, shows this not to be the case. The calculations do therefore indicate that a small N-N expansion of 0.02 Å accompanies the weak chemisorption on the surface. This result agrees rather well with the result obtained by our PhD measurements in which an intramolecular expansion of 0.03 Å was obtained.

The Ni-Ni layer spacing given in table 3.1 for the DFT calculation reflects the systematic error of the DFT result for bulk Ni. The rather large surface layer expansion seen in the DFT calculation must also include a similar 0.03 Å (1.7% of the bulk value of 1.76 Å) component due to this underlying failure to provide a perfect description of the bulk. The DFT results also indicated a remarkably large rumpling (by 0.19 Å) of the outermost Ni layer, but as commented earlier the PhD results are only very weakly sensitive to this parameter so it was not possible to confirm or refute this result experimentally.

The value obtained for the ‘true’ adsorption energy (that is, the difference between the total energy of the equilibrium adsorption phase and the sum of the energies of the isolated N₂ molecule and equilibrium clean surface) was 567 meV per molecule. The energy cost of the rumpling is very small, 75 meV per molecule. Thus, the total adsorption energy determined in this calculation was 642 meV (62 kJ·mol⁻¹), a figure which is certainly larger than the experimental value (around 40-45 kJ·mol⁻¹ at low coverage, but significantly less, 25 kJ·mol⁻¹, at 0.5 ML coverage [41]) but is also much closer to the experimental value than earlier estimates based on calculations of a NiN₂ cluster [26]. It is also important to note that the theoretical calculation is effectively a zero temperature value, and it appears that the surface entropy of this adsorption phase may be unusually large [41]. Notice that if the molecule was fixed in the DFT calculations further from the surface at a Ni-N distance of 2.25 Å as proposed by Moler et al. the adsorption energy was found to be only 11 kJ·mol⁻¹, much lower than the experimental value.

Some insight into the nature of the N₂/Ni bonding is provided by the modification of the spatial redistribution of the electron charge density which can be readily extracted from the results of the DFT calculations. An appropriate charge density *difference* contour map is shown in Fig. 3.8. This figure shows the difference in electron charge density between that of the actual lowest energy adsorption structure and the sum of the charge densities of the Ni(100) slab and an isolated N₂ placed at the same coordinates. The charge density differences thus reflect the effect of the bonding. The region of electron charge accumulation between the Ni surface atom and the inner N atom is characteristic of the formation of a covalent bond. Notice too that there is clearly an increased electron charge in the molecular orbitals of π -symmetry around the two N atoms as may be expected in the standard Blyholder back-bonding picture; increased population of the antibonding $2\pi^*$ states can also be related to the slight increase in N-N distance in the adsorbed molecule seen in these calculations. The charge density difference contour map of Fig. 3.8 is closely similar to that seen in similar calculations for CO bonded on this surface [66],

clearly confirming the chemisorption character of the bonding which is compatible with the reasonably short Ni-N bond length. These charge density contours do not show in detail which electronic states are involved in the electronic rearrangement associated with the bonding.

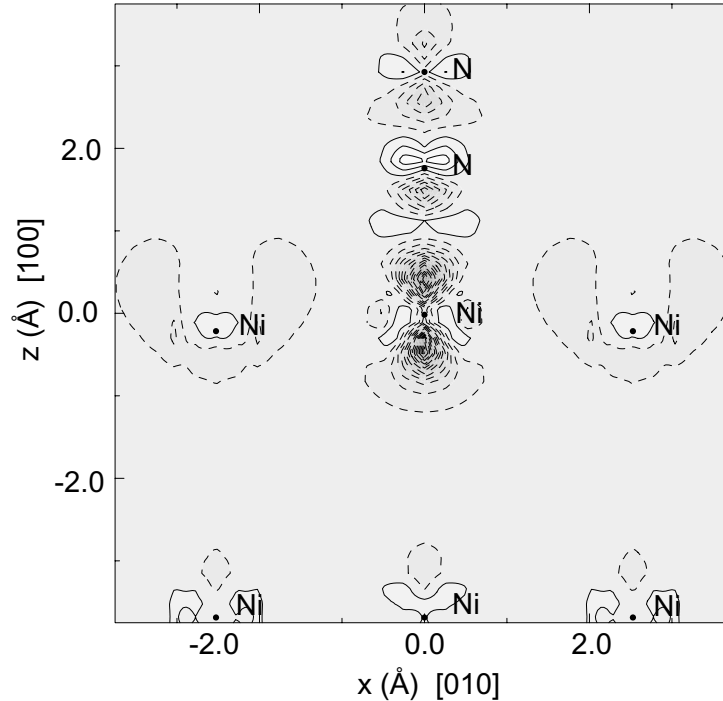


Figure 3.8: Charge density difference contour map for the lowest energy adsorption geometry of N₂ on Ni(100)

3.2 An example of forward focusing

We have already mentioned that the PhD spectra from the outer N atom have a modulation amplitude that appears to be rather large. The outer N is almost 3 Å from the nearest-neighbour Ni backscatterer, so modulations much weaker than for the inner N (which is closer to the substrate) would be expected, unless these modulations are due to scattering off the inner N. However, this is not the case as it is manifested in the image obtained with the projection method for the outer N emitter, where no feature corresponding to the location of the inner N appears. This absence of any sign of the inner N in the projection method image for the outer N emitter has been explained in a previous section in terms of distinct scattering strengths in the backward direction between the inner N and the second nearest Ni neighbour, but the arguments given there do not explain why the Ni atom is so well imaged despite its large distance from the outer N emitter, and thus why the modulation amplitude of the PhD spectra corresponding to the outer N is so large.

In order to provide an explanation of this phenomenon, we have performed scattering calculations for three simple models. First we simulated the modulations due only to the intramolecular scattering by taking into account in the calculations just the two N atoms. In the top of Fig. 3.9 the result of this calculation for normal emission from the outer N along the [001] azimuth is shown superimposed to the experimental PhD spectrum measured at this emission geometry. As may be expected, the scattering from the nearest neighbour inner N atom is quite weak and, because of the short interatomic distance, leads to weak long period oscillations.

The middle curve shows the scattering of the full Ni cluster, where the inner N scatterer has been omitted. As can be seen, the scattering from the Ni atoms alone gives shorter period oscillations, which match quite well in frequency and phase the experimental spectrum. On the other hand, the modulation amplitude is low, consistent with our previous expectations for such a large distance between the outer N emitter and the Ni scatterer. Adding the inner N to this calculation gives the curve at the bottom of the figure, in which an increase of the modulation amplitude up to the experimental value is observed, while the frequency of the oscillations remains the same. This amplitude enhancement can be attributed to the multiple scattering effect of the inner N, “focussing” the photoelectron wavefield emitted from the outer N onto the Ni backscatterer, and thus leading to a very large increase in the resulting backscattering amplitude.

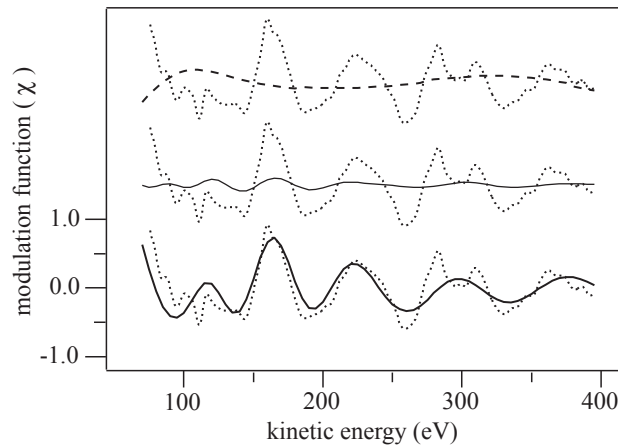


Figure 3.9: Comparison of the experimental normal emission PhD modulation curve from the outer N atom (dotted line) measured along [001] with the results of model calculations as follows: top curve (dashed line) - scattering from the inner N alone; middle curve (thin line) - scattering from the full surface cluster but with the inner N scatterer omitted; bottom curve (thick line) - scattering from the full cluster including the inner N. All calculations include near-neighbour double scattering

Superficially this explanation could appear to be rather surprising, as the PhD technique in the energy-scan mode is actually designed to exploit backscattering since at the typical energy range in which PhD is performed (energies below 500 eV) cross-sections for backscattering are reasonably large. But it should not be forgotten that in this energy

range forward scattering cross-sections are typically even larger. Therefore, the electrons leaving the outer N will also be subject to forward scattering off the inner N, and since true forward scattering does not introduce any pathlength difference, it does not lead to any modulations in the energy-scan spectrum, and it will only influence the relative amplitudes arising from different scattering paths. This is the reason why multiple scattering calculations, including forward scattering events, are essential for a proper interpretation of PhD spectra.

These forward scattering effects are most pronounced for colinear scatterers, and in the present N-N-Ni case they greatly improve the precision of the outer N-Ni distance determination and thus of the intramolecular N-N bond length.

From Fig. 3.9 it can be seen that the result of the simulations performed here for the system consisting of the molecule and the Ni cluster does differ slightly from the full calculations shown in Fig. 3.4. The reason is that in the simulations shown in Fig. 3.9 we have taken into account just forward scattering and near-neighbour double scattering events in order to speed up the calculations.

3.3 Photoemission satellite structure

In chapter 2 we have seen that a core level spectrum not only comprises a spectral peak corresponding to the ionisation of the core level electron to the vacuum, but also some other features that appear at lower kinetic energies than the main line and which are due to the response of the system to the strong perturbation caused by the core ionisation. These features are called satellite structures because their intensity is usually considerably lower than for the main line. In the case of atoms and molecules these satellites are usually described in terms of molecular excitations in the core-hole system, while for solids it is common to distinguish between different types of so called *shake-up* and *shake-off* processes depending on the character of the excitations (see section 2.3). For an adsorbate system the situation is more complicated as in this case there will be a combination of the properties of the free molecule and the solid. Depending on the strength of the interaction established between the molecule and the solid upon adsorption, the excitation process turns out to be rather different. In the case of physisorption, where no chemical interaction between adsorbate and substrate exists, the adsorbed atom or molecule retains many of its gas phase properties, even upon ionisation. On the other hand, when a chemical bond is formed by charge exchange between the adsorbate and the substrate, new final-state relaxation channels open up which are not present in the free atom or molecule and the core hole can be screened completely, like in metals.

In the particular case of simple molecules adsorbed on *d*-metal surfaces, the ionisation of core levels is accompanied by strong many-body effects that are manifested as intense satellite structures that are not present in the photoemission spectra of the corresponding gas phase molecules. The intensity of these satellites depends on the strength of the bonding to the surface. For strong chemisorption, the photoemission spectra from core

levels of these simple molecules contain a broad feature separated by 5-6 eV from an intense main line (e.g. CO/Ni(100) [25], CO/W(110) [67], NO/Ru(001) [68]). For weak chemisorption, this broad feature has a considerably larger intensity than the “main line” (e.g. CO/Cu(100) [69], CO/Ag(110) [70], N₂/Ni(100), N₂/W(110), and N₂/Ru(001) [67]), which resulted in the adoption of the term “giant satellite”.

The first attempts to explain the adsorbate-metal interaction led to two different approaches to the problem. One, originally developed by Schönhammer and Gunnarsson [71, 72], described the interaction by a model Hamiltonian using the idea previously proposed by different authors [73–75] that core-hole screening in adsorbate-metal systems is mainly due to charge transfer from occupied substrate metal bands to an initially unoccupied adsorbate level ($2\pi^*$ in the case of CO and N₂ chemisorption), which is pulled below the Fermi level by the attractive core-hole potential. According to this model, the distribution of the spectral intensity depends on the position of the initially unoccupied adsorbate level in the ionised state and on the degree of hybridisation between adsorbate and substrate, that is, on the strength of adsorption. This model, based on the interaction of discrete adsorbate levels with substrate metal bands, allowed them to predict qualitatively the changes in the intensity of the adsorbate core-hole spectra when going from strongly chemisorbed molecules to cases of weak chemisorption. For strong chemisorption the “fully relaxed” peak or “main line” should dominate the spectrum, while in the weak chemisorption case the peak to appear at higher binding energy, the “satellite”, should carry most of the spectral weight. These predictions were found to compare very well with the experimental data. In these experimental works the peaks were interpreted as “screened” (fully relaxed) and “unscreened” (satellite) final states. However, this “picture” was later criticised [29] as inconsistent with a set of N 1s core hole spectra from N₂ adsorbed on three different transition metals [28] that were found to be very similar despite the substantial differences in the valence density of states of the various substrates.

The other group of models is based on the cluster approach, in which it is assumed that the local metal-molecule interactions are responsible for the spectral function, an idea supported by earlier experimental comparisons between chemisorbed N₂ and dinitrogen-transition-metal complexes that showed strong similarities [76–80]. On the basis of cluster calculations, one can find several mechanisms of core-hole screening for adsorbates on metals (for details see [38] and references therein).

Both kinds of models were applied to the description of the weak chemisorbed system N₂/Ni(100), giving a plethora of different results concerning the electronic ground state of the system, the bonding distance and the screening mechanisms. However, later high-resolution measurements of the N 1s XPS of the N₂/Ni(100) system [30] revealed some new features in the satellite region which were not predicted by any of the theoretical work mentioned above. In order to explain these new characteristics of the spectrum Nilsson et al. [30] exploited the technique of photoelectron diffraction in the high energy forward scattering form (XPD) to separate the spectra into the contributions coming from the two inequivalent N atoms. They showed that the spectrum of the outer nitrogen has a

richer satellite structure than the inner nitrogen. The satellite of the outer N comprises a component at 2.1 eV from the main line and an intense structure at 5.8 eV with a shoulder at 8.5 eV, whereas only one strong peak at 5.3 eV is observed in the inner N satellite. These spectral features were explained by the authors using the equivalent core approximation and by comparison with the C 1s spectra from CO adsorbed on Ni(100). The satellite at 2.1 eV from the main line in the outer N spectrum is interpreted as a shake-up excitation of the $2\pi^*$ orbital. The strong satellites to appear around 5-6 eV in both outer and inner N spectra are assigned to Rydberg-like transitions of the partially occupied $2\pi^*$ orbital into $3s$ -, $3p$ - and $4p$ -derived states. The satellite at 8.5 eV in the outer N spectrum is attributed to 1π - $2\pi^*$ intramolecular shake-up transition.

The first theoretical interpretation of these new features was based on *ab initio* restricted configuration interaction (CI) calculations on the N 1s XPS of the NiN₂ cluster and provided reasonably good agreement with the experimental spectra [33]. Nevertheless, the interpretation of the most intense lines in the spectra given in this theoretical work differs from that proposed by Nilsson. The main line in both separated spectra is suggested to be a σ to σ^* shake-down, rather than π to π^* , and the giant satellites are σ to σ^* shake-up satellites that are close to the Koopmans' states.

The assignment of the satellite remains hitherto controversial. Indeed, some of the most recent theoretical investigations of this satellite structure [38–40] have even questioned the validity of the separation of the N 1s spectrum into inner and outer components. This theoretical work point out that much of the satellite emission is not truly localised in one or other N atom, but involves coherent emission from both sites.

3.3.1 Core-hole localisation

In this work we have measured the complete N 1s photoemission spectrum over a very wide range of emission angles and energies, and these data also contain potentially relevant information concerning the satellite structure which is more related to the electronic structure of this surface. However, our data were not measured at the low photoelectron energies required to observe the near-threshold changes in the satellite structure which might be expected to depend on the electron escape velocity. Furthermore, the spectra collected in our PhD measurements are not intended to have sufficient signal-to-noise ratio to observe relatively fine lineshape changes in different emission direction or energies. On the other hand, if the emission in the satellite states is truly localised on the two inequivalent N atoms, as the work by Nilsson et al. suggests [30], we may hope to learn something from the photoelectron diffraction modulations displayed by the emission from the satellite.

Our intention was to see if the backscattering photoelectron diffraction of the satellite peak would reflect the expected mix of emission from the inner and outer sites. In Fig. 3.10 we show the comparison between the PhD modulation spectra of the broad satellite peak (dashed lines) measured in the [110] azimuth at two different emission angles, 0° and 30° with respect to the surface normal, and the experimental PhD spectra obtained from

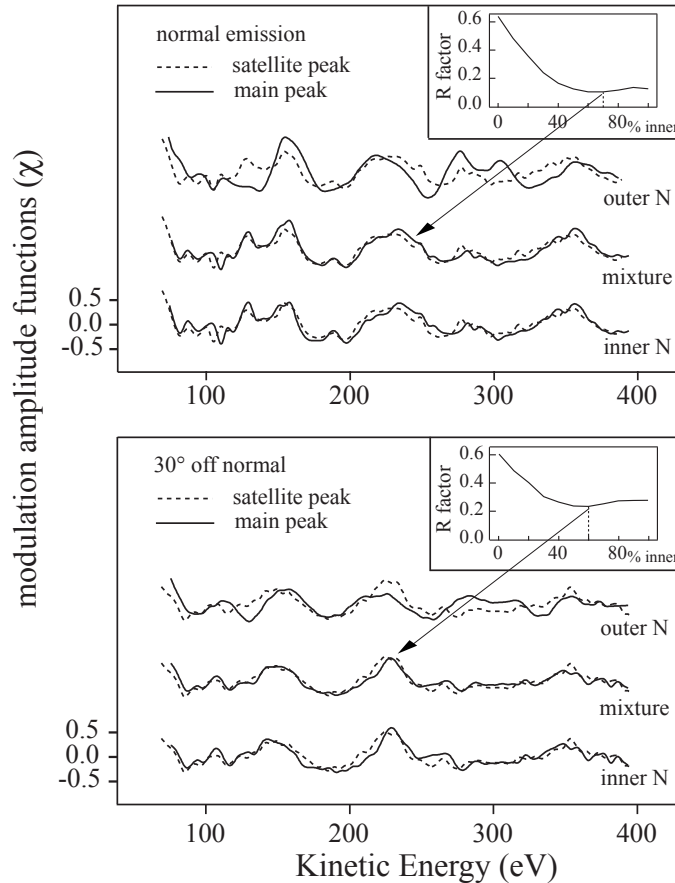


Figure 3.10: Comparison of the PhD modulations spectrum obtained from the main N 1s satellite emission (dashed line) at 0° and 30° emission angle along the [001] azimuth with the spectra obtained from the inner (bottom) and outer (top) N 1s adiabatic peaks at the same geometries. The middle spectra compare the same satellite spectrum with the best-fit simulation obtained by adding the inner and outer N 1s adiabatic emission spectra in different proportions.

the outer and inner N main peaks plus the mixture of the PhD spectra of these two main peaks that gives us the best agreement with the satellite PhD spectrum. The insets in Fig. 3.10 show the variation of this level of agreement as a function of the fraction of each local emitter, evaluated using the same R-factor that we use to compare experimental and simulated spectra as a function of the fraction of each local emitter. For normal emission the contribution of the inner N is around $70(+10/-15)\%$, while at 30° off-normal emission the fraction of the satellite corresponding to emission from the inner N is slightly less, around $60(+14/-20)\%$. Although the R-factor minima are very shallow, it is clear that the fits indicate that at normal emission the PhD modulations showed by the broad satellite peak are dominated by those seen for electrons emitted from the inner N atom. However, for the 30° emission geometry this is less pronounced, and indeed a 1:1 contribution of the two emitters falls well within the precision estimates.

The relative contributions of the two inequivalent N emitter sites to the satellite peak may be influenced by two different factors. Firstly, the emission from the inner N will be forward scattered off the outer N, an effect which will be pronounced at normal emission. Secondly, there are differences in the extent to which the spectral intensity is diverted out of the adiabatic peak and into the many-body excitation spectrum for the two inequivalent N atoms. Although the total photoemission cross-section for the two N atoms should be the same, the fraction of the emission appearing in the adiabatic peak may differ. In order to get a quantitative idea about the way the spectral intensity is distributed into different components for the two inequivalent N atoms, we have performed a simple numerical integration of the published separate extended N 1s spectra. From this we estimate that for the inner N 25% of the intensity appears in the adiabatic peak, 28% is in the broad satellite peak around 6 eV lower in kinetic energy, and 47% appears in the long spectral 'tail' which we assume to be all associated with intrinsic excitations. The corresponding values for the outer N are 20% for the adiabatic component, 37% for the satellite and 43% for the tail.

This greater intensity of the adiabatic emission from the inner N atom is actually seen in our spectra at all emission angles. Due to the strong modulation effects of the photoelectron diffraction present in our data, an exact estimate of the intensity ratio between emission from the inner and the outer N atoms cannot be obtained. However, the data shown in Fig. 3.11 provide a reasonably clear indication of the underlying trend of the average intensity ratio in the absence of these interference effects. In this figure the ratio of the intensity of the inner to outer N adiabatic peaks is shown as a function of photoelectron energy for different emission angles. Strong modulations, especially near normal emission, are seen due to photoelectron diffraction. Nevertheless the superimposed straight lines give a guide to the underlying trend of the average intensity ratio in the absence of these interference effects. At normal emission the intensity of the inner N peak is greater than that of the outer N by more than a factor of 2.5, value which is reduced with increasing emission angle as one moves away from the forward scattering condition. However, even at the higher angles, well away from the forward scattering geometry, the average ratio is around 1.3, very similar to the 25:20 adiabatic peak ratio deduced from the complete spectral separation using XPD mentioned above. Therefore our data confirm that the outer N photoemission has less spectral intensity in the adiabatic emission peak than that of the inner N.

The fact that the emission from the inner N has more spectral intensity in the adiabatic peak implies that there is less spectral intensity in the many-electron part of the spectrum, and indeed, according to the XPD separation, there is less spectral intensity in the satellite peak component. This means that in the absence of forward scattering, which should influence the normal emission satellite PhD spectrum, but not that recorded at 30°, one would expect the outer N to contribute more than 50%, specifically about 57% (37% outer:28% inner) to the intensity of the satellite and thus also to its PhD modulations. Instead of that we found a 40(+20/-14)% contribution, but the expected 57% does lie within the estimated precision. These data are therefore formally consistent with the

analysis of both the XPD and the PhD data based on the assumption that the satellite peak is separable into components fully localised on the two inequivalent N atoms.

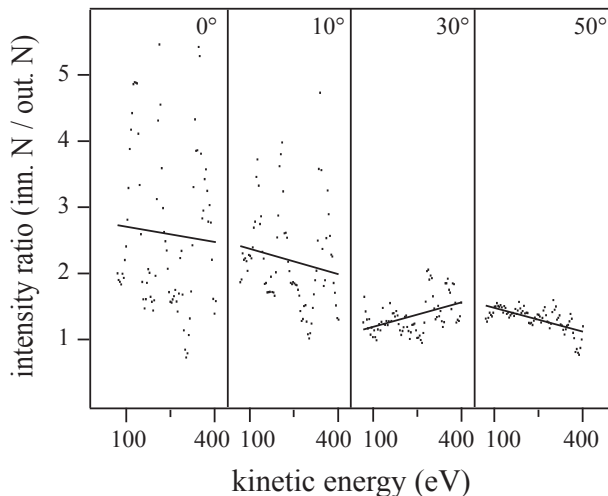


Figure 3.11: The ratio of the intensity of the inner to outer N adiabatic photoemission peaks as a function of photoelectron energy for emission angles of 0° , 10° , 30° , 50° . The superimposed straight lines provide a guide to the underlying trend of the average intensity ratio in the absence of the photoelectron diffraction modulations.

3.4 General discussion and conclusions

The present structure determination of the Ni(100)*c*(2x2)-N₂ system corroborates the previously widely assumed qualitative structure for this phase. However, the Ni-N bond length found in this experimental study, 1.81 ± 0.02 Å, is in strong disagreement with the previously published value of 2.25 Å obtained by Moler et al., and therefore also with the idea that associates very large bond lengths with weak chemisorption bonds. This controversy raises an interesting question regarding the true nature of the N₂/Ni(100) surface bonding. Indeed, a direct comparison with the bond distances showed by other weakly chemisorbed systems which involve N adsorption on atop sites, e.g. NH₃ on Ni(111), 1.97 Å [81], and on Ni(100) 2.01 Å [82], or pyridine (C₅H₅N) on Ni(111), 1.97 Å [83], might reasonably cause us to question the conventional labelling of the Ni(100)/N₂ bonding as “weak chemisorption”. From the point of view of the electronic structure, the question of the nature of the bonding has been discussed in the context of valence band photoemission [25] and X-ray emission spectroscopies [60, 61], but unfortunately these studies do not provide any information about bond lengths. One possible explanation to this apparent dilemma could be that while the Ni(100)/N₂ bonding could be in fact strong, the adsorption may involve some large energy cost in structural modification which produces an overall adsorption energy which is low. This is actually the case for

the adsorption of acetylene (C₂H₂) on Cu(111) [84, 85]. Despite the fact that acetylene desorbs from this surface at temperatures well below room temperature, the bonding to the substrate is strong, but the large energy cost of the molecular modification produced upon adsorption, which causes a large increase in the C-C bondlength, leads to an overall adsorption energy which is low. For N₂ adsorbed on Ni(100), however, any expansion of the N-N distance seems to be rather modest and not sufficient to clarify the dilemma. Moreover, DFT calculations show that the adsorption energy is indeed low, and that the energy cost associated with the rumpling of the surface upon adsorption counts only for a marginal 13 % of the total adsorption energy.

This apparent lack of direct relationship between bond length and bond strength seems to be also the case for the Ni(100)-c(2x2)-H/CO coadsorbed system, where CO occupies also the atop site. While the adsorption energy for this system appears to be at least a factor of two less than for the simple Ni(100)c(2x2)/CO phase, in which CO is also in an atop adsorption site, the Ni-C bond length extension observed when going from the strong chemisorbed CO on Ni(100) to the weak chemisorbed H/CO is only 0.06 Å, much less than the change associated with a halving of the bond order(0.15 Å) [66, 86].

The value of the Ni-N bond distance obtained here is an important piece of structural information which will should have be considered in any future theoretical description of N₂/Ni(100) chemical bonding. Actually, it clearly invalidates those models implying large molecule-substrate bond distances, such as the one proposed by Brundle et al. [25] where a bondlength of 2.27 Å was used.

Regarding the broad satellite present in the N 1s photoemission spectrum at around 6 eV from the adiabatic peaks, we have found that its PhD modulations could be separated into contributions from the inner and outer N atoms, suggesting that the emission in the satellite states is largely localised on these two inequivalent N atoms, as Nilsson and coworkers have previously proposed [30]. Although the precision with which we can make this statement is clearly limited, the extent of the delocalisation claimed by the theoretical work of Dobrodey and coworkers [38–40], appears to be rather limited.